Precise Evaluation of the Electron $(g-2)$ at 4 loops: The Algebraic Way

Pierpaolo Mastrolia[1] and Ettore Remiddi[1,2]

[1] Dipartimento di Fisica, Università di Bologna
[2] INFN, Sezione di Bologna, Italy

Abstract. It is expected that the next generation of $(g-2)$ experiments will pin down the error below the 1ppb (parts per billion) level; to cope with such a precision, the current error on the theoretical value of the 4 loop QED contribution must be reduced by at least a factor ten. To avoid the rounding problems which affect the numerical calculation, we developped and implemented as computer code various exact algebraic algorithms for reducing the very many integrals appearing in the calculation to a much smaller number of master integrals.

1 The Current Status of the Theory

The electron magnetic anomaly a_e, related to the gyromagnetic ratio g_e through the relation $a_e = (g_e - 2)/2$, is experimentally known with an error of 4 ppb (parts per billions), which is expected to be reduced by at least an order of magnitude in the next generation experiments (see the review paper by Kinoshita [1] in this book for more details). The current theoretical error is of the order of 1 ppb, and is dominated by the error in the numerical evaluation of the 4 loop QED contribution. To avoid the rounding problems which affect the numerical evaluation [1] we are developping an algebraic approach to the problem, whose basic idea is to reduce, as a first step, the very many integrals (perhaps a few dozens of millions) occurring in the calculation to a much smaller number (hopefully a few hundred, but the exact number is not yet known) of socalled "master integrals" by means of exact, algebraic manipulations free of any rounding error. As any set of linearly independent integrals can be choosen as master integrals, the freedom which is left in their choice can be exploited to pick up the numerically best behaved integrals for the a fast and precise numerical evaluation – or even for attempting the exact analytic integration of some of them (a completely analytic evaluation is a much more difficult task).

The next theoretical error will then be the 5 loop QED contribution, expected to be a few units times 0.06 ppb; while nothing is known of the convergence of the perturbative expansion of QED, there is sofar no evidence for a bad convergence in the case of $a_e(\mathrm{th})$. Finally, the error in the hadronic contribution is still somewhat smaller (less than 0.03 ppb).

2 Feynman Amplitudes for the $g-2$ and the Integration by Parts Identities

The basic ingredient of our approach is the systematic exploitation of the Integration by Parts Identities (IBPI's [2]) for the reduction of all the occurring integrals to the master integrals. In a previos paper [3] (carrying the same title as the present paper) we have presented a highly automatized procedure for solving the IBPI's for any given "topology" (in practice any combination of Feynman propagators). We will discuss here the algorithms developped and implemented for the automated generation of all the relevant topologies and the corresponding IBPI's; the algorithms apply, practically without changes, not only to the magnetic anomaly but also to any other static quantity, such as the renormalization counterterms and the slope of the charge form factor.

Automated procedures are needed because the number of vertex Feynman graphs (and hence also of all their substructure or "subtopologies") which must be evaluated in perturbative QED for obtaining $a_e(\text{th})$ grows quickly with the order of perturbation theory (or, which is the same, with the number of loops) and is too large to be evaluated by hand. For the computer processing of the algebra we rely on the algebraic program `FORM`, by J. Vermaseren [4]; for writing the `FORM` code relevant to the various subtopologies we developped a number of *ad hoc* programs (written in `C`) which read in input a concise description of any of the subtopologies and then write in output a piece of the `FORM` code which corresponds to that subtopology.

The 7 Feynman graps for the QED vertex with 2-loop are shown in Fig. 1. They correspond to a process in which the external electromagnetic field ex-

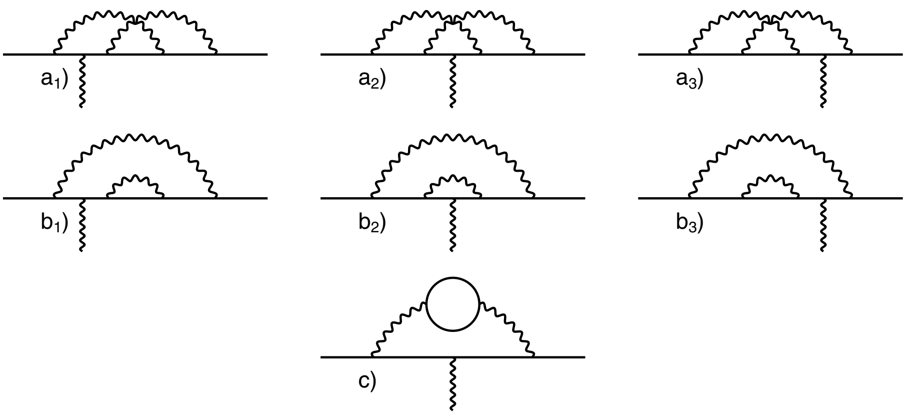

Fig. 1. The 2-loop vertex graphs

changes a momentum Δ_μ with the electron. The $a_e(\text{th})$ is extracted from the vertex amplitude by means of a suitable projector (whose explicit expression will

Search Hits Help

not be given here) in the static limit $\Delta_\mu \to 0$. Once the static limit is taken, one is left with a combination of self-mass like amplitudes (*i.e.* an amplitude for the electron-electron transition) in which Δ_μ has disappeared. It is then natural to group together in a single self-mass like amplitude all the vertex graphs corresponding to a same self-mass in the static limit; the 3 vertex graphs $\mathtt{a}_1, \mathtt{a}_2, \mathtt{a}_3$ of Fig. 1, for instance, correspond to the self-mass graph of Fig. 2a) below, and the whole set of 7 2-loop vertex graphs correspond to a total of 3 self-mass amplitudes, shown in Fig. 2.

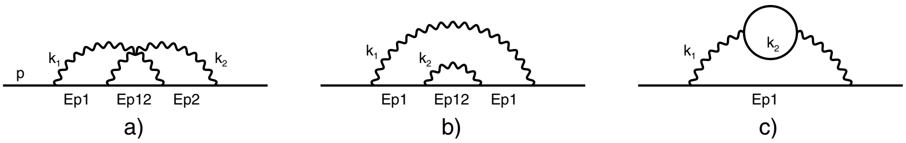

Fig. 2. The 2-loop self-mass graphs

In all the above 2-loop graphs one has the external momentum p, which satisfies the mass-shell constraint $p^2 = -m_e^2$, m_e being the mass of the electron, and 2 loop momenta, k_1 and k_2; with them one can form the 5 scalar products k_1^2, k_2^2, $(p.k_1)$, $(p.k_2)$, $(k_1.k_2)$. Any of the occurring graphs involves a subset of the following Feynman propagators (more exactly: inverse Feynman propagators in the momentum representation)

$$\begin{cases} \mathtt{K1} &= k_1^2 \ , \\ \mathtt{E1} &= k_1^2 + m_e^2 \ , \\ \mathtt{Ep1} &= (p-k_1)^2 + m_e^2 \ , \\ \mathtt{K2} &= k_2^2 \ , \\ \mathtt{E2} &= k_2^2 + m_e^2 \ , \\ \mathtt{E12} &= (k_1-k_2)^2 + m_e^2 \ , \\ \mathtt{Ep2} &= (p-k_2)^2 + m_e^2 \ , \\ \mathtt{Ep12} &= (p-k_1-k_2)^2 + m_e^2 \ . \end{cases} \tag{1}$$

After the projection, $a_e(\mathrm{th})$ has the form of a sum of many integrals (of the order of one hundred for any graph at 2-loop, perhaps 10^l at l loops), each integral being a product of powers of the scalar products divided powers of the propagators occurring in the graph; note that the projection involves also some differentiation with respect to the momentum transfer Δ, so that the actual powers of the propagators can be higher than in the original graph.

It is clear that propagators and scalar products are not linearly independent, so that one can express some of the scalar products in terms of the propagators which are present in the graph (this procedure is sometines calles trivial tensor reduction). To make a simple example, if `K1` and `Ep1` are present, one can write the obvious identity

$$\frac{(p.k_1)}{\mathtt{K1}\ \mathtt{Ep1}} = \frac{1}{2\ \mathtt{K1}} - \frac{1}{2\ \mathtt{Ep1}} \ . \tag{2}$$

In so doing, some of the propagators can disappear; in the case of the double cross graphs of Fig. 2a), the disappearance of a single propagator leads to the appearance of the five substructures of Fig. 3.

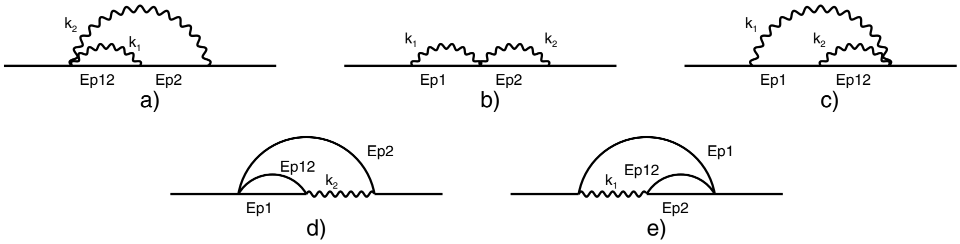

Fig. 3. The substructures of the double cross graphs

It is clear that not all the substructures are independent: the substructure of Fig. 3a), for instance, goes into Fig.. 3c) with the exchange of the loop variables $k_1 \leftrightarrow k_2$. and the same is true for the substructures of Fig. 3d) and 3e). But also the structure of Fig. 2b) is easily seen to be identical to the structure of Fig. 3c) – indeed, it involves exactly the same propagators $\mathtt{K1}, \mathtt{Ep1}, \mathtt{K2}, \mathtt{Ep12}$ (the powers of the single propagators don't matter). Similarly, the third selfmass graph, Fig. 2c), which involves the propagators $\mathtt{K1}, \mathtt{Ep1}, \mathtt{E2}, \mathtt{E12}$, has a structure equivalent to Fig. 3e), which involves $\mathtt{K1}, \mathtt{Ep1}, \mathtt{Ep2}, \mathtt{Ep12}$, as shown by the shift of the loop momentum $k_2 \to p - k_2$. It is so apparent that what really matters is not the set of the separate Feynman graphs but the set of all their substructures, which are somehow the "building blocks" of the calculation. Continuing in the process of the trivial tensor reduction also for the substructures of Fig. 3, one finds the further independent substructures (or topologies) shown in Fig. 4; note the appearance of the vacuum amplitudes 4e) and 4f).

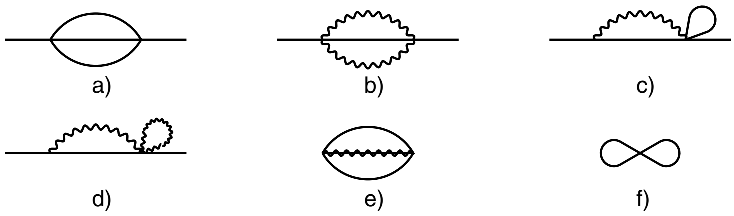

Fig. 4. The completion of the independent 2-loop substructures

For each 2-loop substructure, having say p propagators, one has then to express p of the 5 scalar products in term of the propagators, selecting at the same time $5-p$ scalar products as independent (there can be some arbitrareness in the choice, but the number is fixed). When the choice is made, one can write down explicitly the most general Feynman integral for that substructure/topology, having in the denominator any (integer) power of the occurring propagators, and in the numerator any (positive or vanishing) power of the independent scalar products. In the case of the topology of Fig. 4a), for instance, the propagators after a suitable shift of the loop momenta can be choosen to be `E1, E2` and `Ep12`, and the independent scalar products $(p.k_1)$ and $(p.k_2)$, so that the correspondent Feynman integrals can be written in the form

$$F(4a; a_1, a_2, a_3; b_1, b_2) = (-i)^2 \int \frac{d^d k_1}{4\pi^2} \int \frac{d^d k_2}{4\pi^2} \frac{(p.k_1)^{b_1} \, (p.k_2)^{b_2}}{\mathtt{E1}^{a_1} \, \mathtt{E2}^{a_2} \, \mathtt{Ep12}^{a_3}} \ ,$$

with $a_i \geq 1$, $b_i \geq 0$. Note that for other 2-loop topologies the number of the denominators (the a-indices) can vary, but the sum of the a-indices and the b-indices is always equal to 5 (the number of the independent scalar products at 2 loops).

Once the Feynman integrals are properly defined, one can run for them the IBPI-algorithm described in [3] for expressing all of them in as few as possible master integrals. It can be convenient (but by no means necessary) to proceed in two steps, first expressing integrals with $b_i \geq 1$ in terms of integrals with all the b-indices equal to zero (socalled non-trivial tensor reduction), then expressing integrals with higher values of the a_i in terms of integrals with lower values. Some cases are trivial, as the topology of Fig. 4d), which vanishes as it contains as a factor the massless tadpole

$$(-i) \int \frac{d^d k_1}{4\pi^2} \, \frac{1}{k_1^2} \ ;$$

some cases are simple, as Fig. 3b) which factorizes into two 1-loop amplitudes; other topologies, such as for instance Fig. 2a), have no master integral of their own, *i.e.* all their integrals can be expressed in terms of integrals of simpler topologies (involving less propagators). As a final results, one finds that all the 2-loop integrals can be expressed in terms of just 3 master integrals at two loops, corresponding to the amplitudes of Fig. 4a,4b), with $a_i = 1$ and $b_i = 0$, and Fig. 4f); the last case is particularly simple, as it corresponds to the square of the 1-loop massive tadpole

$$T(d, m_e) = (-i) \int \frac{d^d k_1}{4\pi^2} \, \frac{1}{k_1^2 + m_e^2} = C(d) \, \frac{m_e^{d-2}}{(d-2)(d-4)} \ ,$$

where $C(d)$ is a normalization constant satisfying $C(4) = 1$ but whose explicit expression is otherwise irrelevant for physical quantities, finite in the $d \to 4$ limit. It is to be observed, however, that the tadpole has a polar singularity $1/(d-4)$; when it appears as a factor in some substructure, as in Fig. 4c), the amplitude which multiplies it must be expanded in $(d-4)$ to get the required finite result.

3 Feynman Graphs, Subtopologies and Master Integrals

One can try to organize the calculation along the same pattern also for the 3 and 4 loops, in which case however the number of Feynman graphs and related substructures (or topologies) is much greater: there are indeed 72 Feynman graphs at 3 loops, 891 at 4 loops. Especially in the 4 loops case, it is therefore mandatory to automatize strongly the reduction of all the integrals to the master integrals. To that aim, we begin by preparing (by hand) a first file, whose content is equivalent to Eq.(1) at 2 loops, containing the description of all the possible propagators which will appear in the calculation. Another file, also written by hand, contains the description, in terms of the propagators of the first file, of all the "complete" self-mass graphs, *i.e.* of those graphs which have the maximum allowed number of propagators for the given number of loops and are not substructures of other graphs: at 2 loops Fig.2a), with 5 different propagators, is the only complete graph, at 3 loops there are 4 complete graphs with 8 different propagators, at 4 loops 25 complete graphs with 11 different propagators.

A first program peforms the simple task of reading the two files and generating a file with the list of all the substructures (or topologies) obtained by the complete graphs by removing, in all possible ways, one of the propagators. A second program, the bulk of the procedure, reads the list generated by the first program and checks, one by one, whether any of the topologies is equivalent to some of the topologies already encountered in the list, as 2-loop example is given by the equivalence of Fig. 2b) and Fig. 3c), or to the product of two (or more) simpler topologies with a lower number of loops, such as the 2-loop examples Fig. 3b,3c). For any of the topologies found to be equivalent to some previously encountered reference topology, the program writes a portion of `FORM` code performing the suitable change of loop variables which makes the equivalent topology identical to the reference topology, while the non equivalent topologies are listed in another file.

A last program reads the file of the reference topologies and for each encountered topology writes a portion of `FORM` code performing the trivial tensor reduction.

In so doing, starting from the complete structure, having say n propagtors, one obtains among the rest the list of all the independent topologies with $n-1$ propagators; the procedure is iterated starting again from the independent topologies with $n-1$ propagators, obtaining the list of the independent topologies with $n-2$ propagators and so on, till the topologies with the minimum number of allowed propagators (which is the number of loops; correspondingly one has only the graph consisting of as many tadpoles as the number of loops).

The numbers of the various topologies occurring in the 3-loop case is given in Table 1. It is to be observed that even if there are alltogether 60 independent topologies, the IBPI's reduce all the corresponding integrals to 18 master integrals only.

As already said, at 4 loops there are 25 complete graphs with 11 different propagators, 17 of which without internal electron loops. The numbers of all the generated and independent topologies encountered when processing that

Table 1. 3-loop topologies

number of propagators	generated topologies	independent topologies
8	4	4
7	32	15
6	105	25
5	150	12
4	60	4
total	351	60

significant subset of 17 complete graphs are shown in Table 2 (we expect that most of the subtopologies generated when processing the remaining 8 complete graphs with electron loops will overlap with the subtopologies of the complete graphs without electron loops, as in the 2 and 3 loop case).

Table 2. 4 loop substructures

number of propagators	generated topologies	independent topologies
11	17	17
10	187	93
9	930	235
8	2115	252
7	2016	128
6	896	28
5	168	5
total	6326	758

The reduction of the Feynman integrals to the master integrals with the method described above has just started, so that the total number of the master integrals in the 4 loop case can't as yet be guessed – one can only say that for those 17 complete graphs it is less than 758 ! As preliminary results, we find that all the 5 5-propagator topologies (two of them being actually vacuum amplitudes) give rise to independent master integrals, while some of the 6-propagator topologies do not. To give some examples of simple (but not trivial!) reduction to master integral at 4-loop, let us consider the graph of Fig. 5, which we identify with the label #40501 (standing for: 4 loops, 05 propagators, 01 in that class of graphs).

Defining, for short

$$\mathcal{D}k(\#40501) = (-i)^4 \, \frac{1}{(4\pi^2)^4} \, \frac{d^dk_1 \; d^dk_2 \; d^dk_3 \; d^dk_4}{k_1^2 \; k_2^2 \; k_3^2 \; k_4^2 \; [(p-k_1-k_2-k_3-k_4)^2 + m_e^2]} \; ,$$

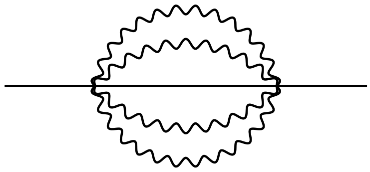

Fig. 5. The 4-loop graph #40501

we find, among the many others, the equations

$$\int \mathcal{D}k(\#40501)\ \frac{(k_1.k_3)}{[(p-k_1-k_2-k_3-k_4)^2+m_e^2]} = \frac{4d-9}{12}\int \mathcal{D}k(\#40501)\ ,$$

and

$$\int \mathcal{D}k(\#40501)\ (k_2.k_4) = m_e^2\ \frac{7-4d}{15(d-2)}\int \mathcal{D}k(\#40501)\ .$$

Similar (but in general much more complicated) formulae have been found for several other cases, but is is still too early to try to estimate how long it will take for obtaining the completion of the reduction of all the integrals to the master integrals.

References

1. T. Kinoshita: *this edition*, pp. 157– 175
2. F.V. Tkachov: Phys. Lett. B **100**, 65 (1981); K. G. Chetyrkin and F.V. Tkachov: Nucl. Phys. B **192**, 159 (1981)
3. P. Mastrolia and E. Remiddi: Nucl. Phys. B (Proc. Suppl.) **89**, 76 (2000)
4. J. A. M. Vermaseren: Symbolic Manipulation with FORM, Version 2, CAN, Amsterdam, 1991